

The Rotational and Gravitational Signature of Recent Great Earthquakes

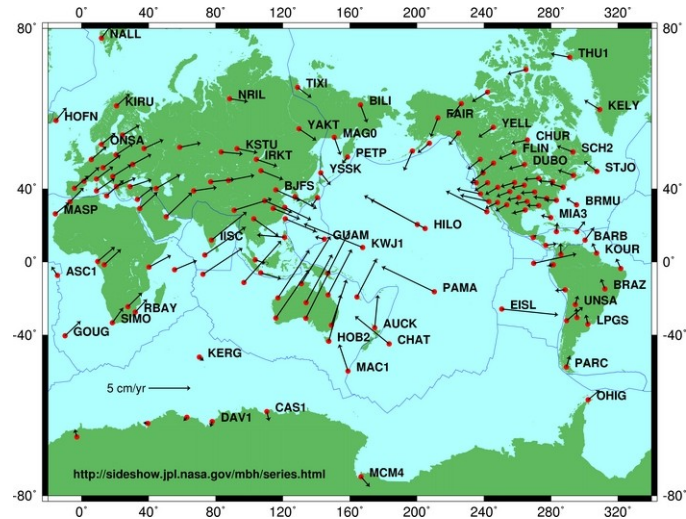
Richard S. Gross

Jet Propulsion Laboratory
California Institute of Technology
Pasadena, CA 91109–8099, USA

7th IVS General Meeting

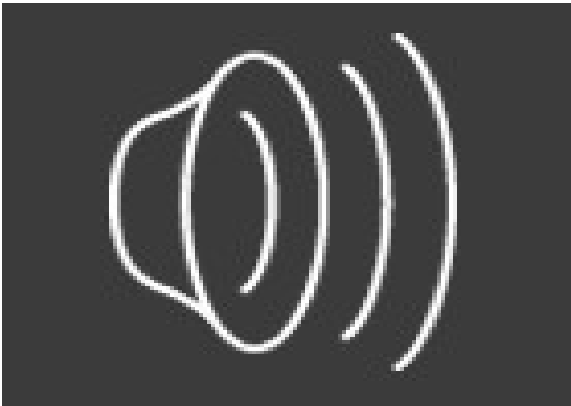
March 4–9, 2012
Madrid, Spain

The Three Pillars of Geodesy

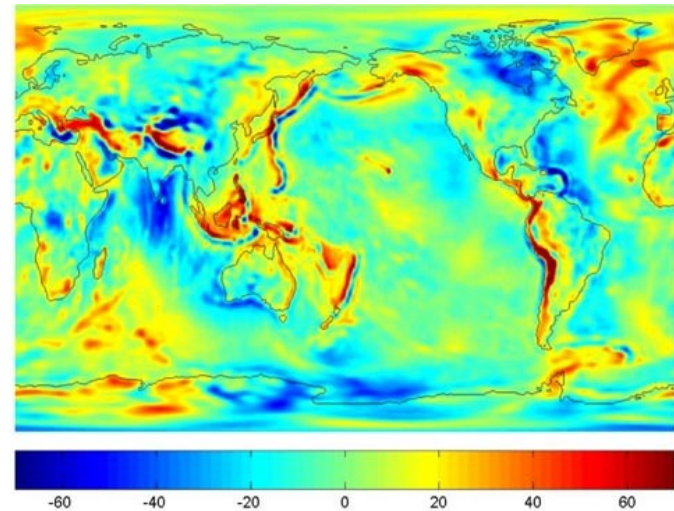


Shape & Deformation

Earth Rotation



Gravity & Geoid



Introduction

- The three pillars of geodesy
 - Geometric shape, rotation, and gravity
 - Static and time varying
- Are related by common observing systems
 - Examples: SLR, GPS, DORIS, VLBI (shape and rotation)
- Are related by common sources of excitation
 - Examples: atmosphere, oceans, hydrology, earthquakes, GIA
- But are sometimes modeled separately
 - Example: flat Earth models for earthquake displacements, spherical Earth models for rotation
- A unified modeling approach
 - Allows excitation process to be studied using all geodetic data
 - Example: earthquakes

Geodetic Effects of Earthquakes

- Flat Earth models
 - Commonly used to model site displacements
 - May or may not include effects of layering
 - Do not include effects of sphericity
 - Important for great earthquakes having rupture lengths of 1000 km (10°) or more
- Spherical Earth models
 - Commonly used for rotation effects
 - Often used for gravity effects
- A unified mode sum approach
 - Based on a realistic Earth model (PREM)
 - Automatically accounts for effects of sphericity, layering, self-gravitation

Site Displacements

- Equation of motion

$$\nabla \cdot \boldsymbol{\tau} + \mathbf{f}_g + \mathbf{f}_s = \rho(\mathbf{r}) \frac{\partial^2 \mathbf{u}}{\partial t^2}$$

- Solve by expanding displacement field

$$\mathbf{u}(\mathbf{r}, t) = \sum_k a_k(t) \mathbf{u}_k^*(\mathbf{r})$$

- Normal mode eigenfunctions

$$\mathbf{u}_k(\mathbf{r}) = {}_n U_l(r) Y_{lm}(\theta, \lambda) \hat{\mathbf{r}} + {}_n V_l(r) \frac{\partial Y_{lm}}{\partial \theta} \hat{\boldsymbol{\theta}} + {}_n V_l(r) \frac{1}{\sin \theta} \frac{\partial Y_{lm}}{\partial \lambda} \hat{\boldsymbol{\lambda}}$$

- Expansion coefficients (static limit)

$$a_k(\infty) = \frac{M_o}{\omega_k^2} \hat{\mathbf{M}} : \boldsymbol{\varepsilon}_k(\mathbf{r}_s)$$

- Normal mode eigenfrequencies and eigenfunctions

- Computed using MINOS program provided by Guy Masters

Earth Rotation

- Conservation of angular momentum
 - Earthquakes are internal to the Earth (no load Love numbers)
 - Earthquakes occur suddenly (motion effects neglected)
- Length of day

$$\frac{\Delta\Lambda(t)}{\Lambda(t)} = \frac{\Delta I_{zz}(t)}{I_{zz}^{(m)}}$$

- Polar motion excitation

$$\Delta\chi_x(t) + i\Delta\chi_y(t) = \frac{1.61}{I_{zz} - I_{xx}} [\Delta I_{xz}(t) + i\Delta I_{yz}(t)]$$

- Inertia tensor

$$\mathbf{I} = \int \rho(\mathbf{r}) [(\mathbf{r}\cdot\mathbf{r})\mathbf{I} - \mathbf{r}\mathbf{r}] dV$$

- Perturbed inertia tensor ($\mathbf{r} \Rightarrow \mathbf{r} + \mathbf{u}$)

$$\Delta\mathbf{I} = \int \rho_o(\mathbf{r}) [2(\mathbf{r}\cdot\mathbf{u})\mathbf{I} - (\mathbf{u}\mathbf{r} + \mathbf{r}\mathbf{u})] dV$$

Gravitational Field

- Gravitational potential of Earth

$$U(\mathbf{r}) = \frac{GM}{r} \sum_{l=0}^{\infty} \sum_{m=0}^l \left(\frac{a}{r}\right)^l [C_{lm} \cos m\lambda + S_{lm} \sin m\lambda] \tilde{P}_{lm}(\cos \theta)$$

- Stokes coefficients

$$C_{lm} + iS_{lm} = \frac{N_{lm}}{Ma^l} \int_{V_o} r^l Y_{lm}(\theta, \lambda) \rho(\mathbf{r}) dV$$

- Perturbed Stokes coefficients ($\mathbf{r} \Rightarrow \mathbf{r} + \mathbf{u}$)

$$\Delta C_{lm} + i \Delta S_{lm} = \frac{N_{lm}}{Ma^l} \int_{V_o} r^{l-1} \mathbf{u} \cdot (\hat{\mathbf{r}} l + \nabla_h) Y_{lm}(\theta, \lambda) \rho(\mathbf{r}) dV$$

Earth Rotation & Gravitational Field

- Related via the inertia tensor

- Elements of inertia tensor are related to the degree-2 Stokes coefficients

$$I_{xz} = -\sqrt{5/3} M a^2 C_{21}$$

$$I_{yz} = -\sqrt{5/3} M a^2 S_{21}$$

$$I_{zz} = \frac{1}{3} [T - \sqrt{20} M a^2 C_{20}]$$

- Trace of inertia tensor

$$T = 2 \int \rho(\mathbf{r}) r^2 dV$$

- Perturbed trace of inertia tensor ($\mathbf{r} \Rightarrow \mathbf{r} + \mathbf{u}$)

$$\Delta T = 4 \int \rho_o(\mathbf{r}) \mathbf{r} \cdot \mathbf{u} dV$$

Polar Motion Excitation

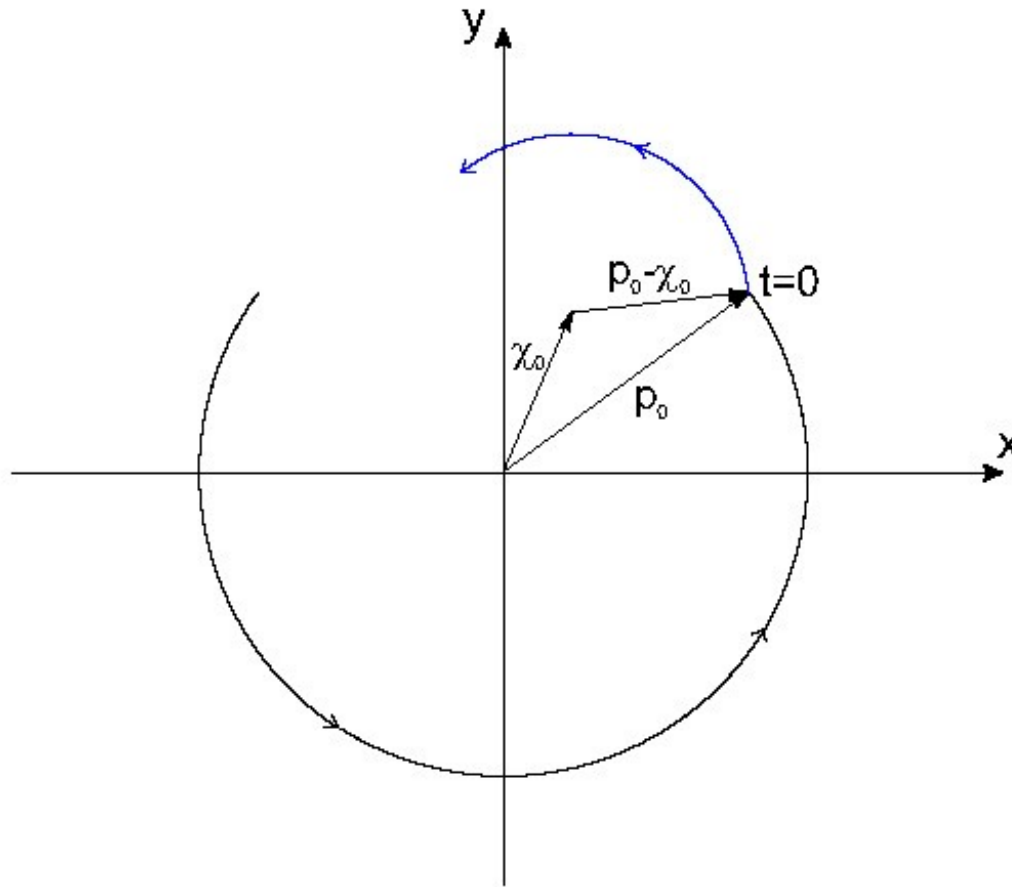


Figure 2: Excitation of polar motion by the step function.

Recent Great Earthquakes

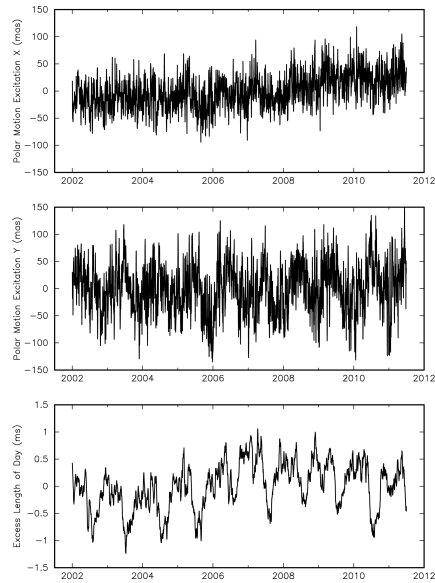
- 2004 Sumatra ($M_w = 9.3$)
 - 5 sub-event model of *Tsai et al. (2005)*
 - Based on seismic data
- 2005 North Sumatra ($M_w = 8.5$)
 - Caltech's Tectonics Observatory slip model with 295 patches
 - Based on GPS, seismic, and coral uplift and subsidence data
- 2007 South Sumatra ($M_w = 8.4$)
 - Caltech's Tectonics Observatory slip model with 203 patches
 - Based on GPS, seismic, and InSAR data
- 2010 Chile ($M_w = 8.8$)
 - Updated USGS slip model with 166 fault patches slipping
 - Based on seismic data
- 2011 Japan ($M_w = 9.0$)
 - Updated USGS slip model with 319 fault patches slipping
 - Based on seismic data

Modeled Change in Earth Rotation

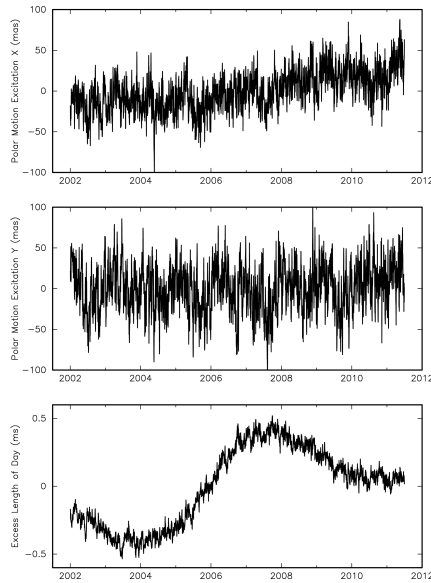
	ΔIod (μsec)	$\Delta\chi_x$ (mas)	$\Delta\chi_y$ (mas)
<i>Recent great earthquakes</i>			
2004 Sumatra ($M_w = 9.3$)	-6.77	-1.41	1.85
2005 North Sumatra ($M_w = 8.5$)	-0.84	-0.25	0.08
2007 South Sumatra ($M_w = 8.4$)	-0.64	-0.17	-0.07
2010 Chile ($M_w = 8.8$)	-1.71	-1.38	3.26
2011 Japan ($M_w = 9.0$)	-1.36	-2.97	3.27
<i>Approximate measurement uncertainty (1σ)</i>	10	5	5
<i>Other great earthquakes</i>			
1960 Chile ($M_w = 9.5$; Chao & Gross, 1987)	-8.40	-9.53	20.45
1964 Alaska ($M_w = 9.2$; Chao & Gross, 1987)	6.79	-7.11	-2.31

Observed Residual Excitation (2002.0 – 2011.5)

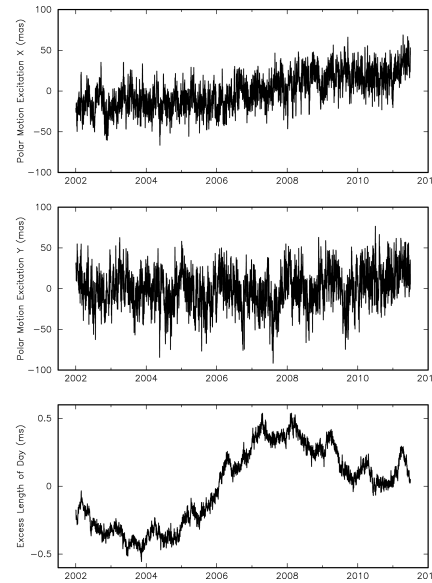
observed



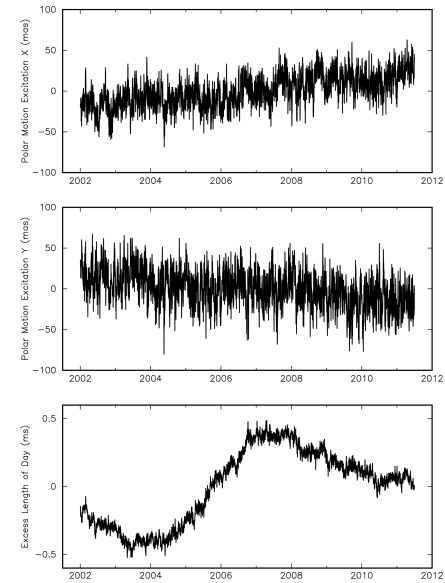
obs-atm



obs-atm-ocn



obs-atm-ocn-hyd



Variance (percent reduction)

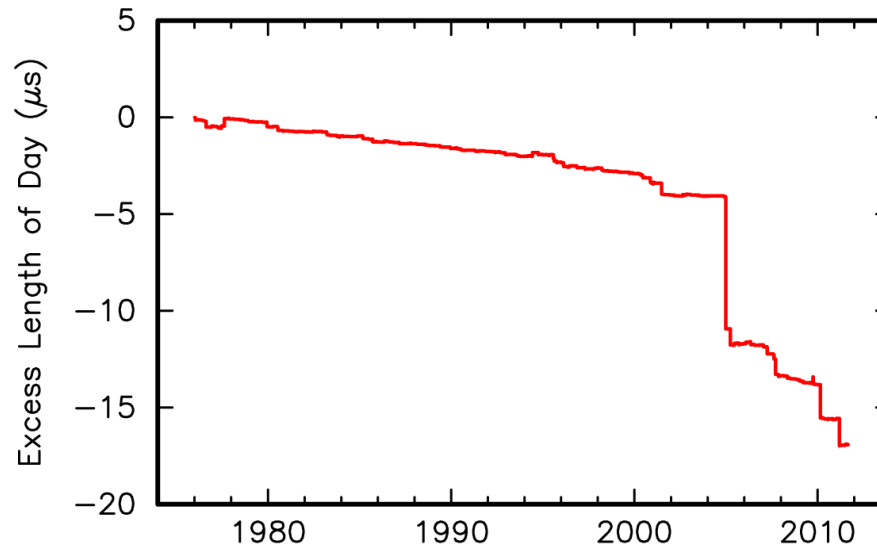
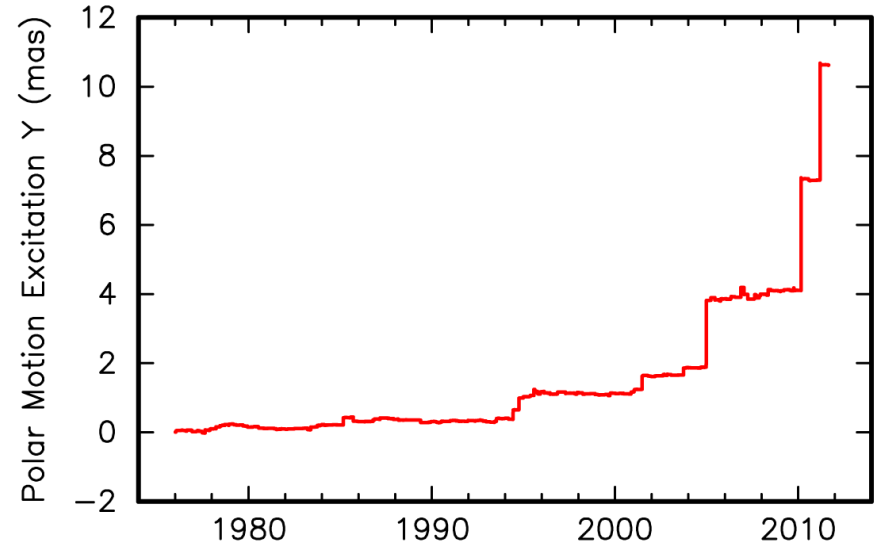
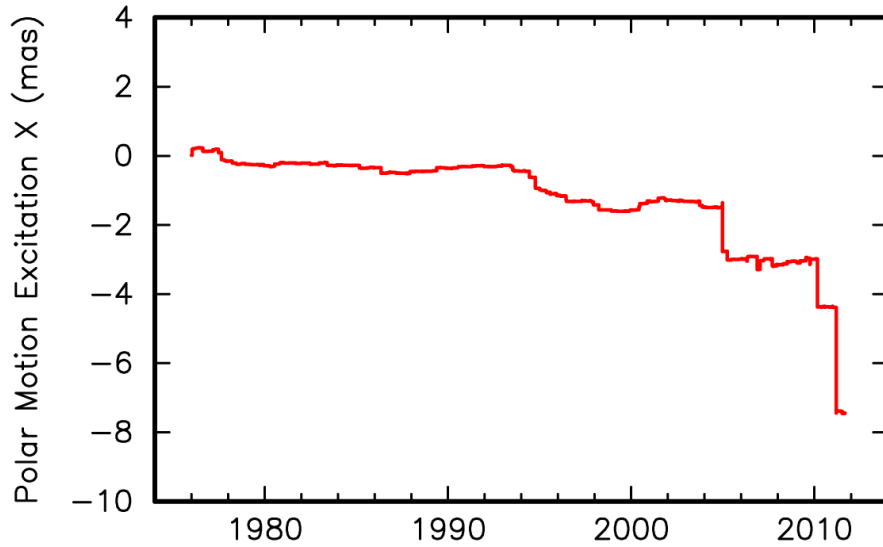
chi-x: 912 mas²
 chi-y: 1978 mas²
 lod: 0.185 ms²

564 mas² (38%)
 841 mas² (57%)
 0.0798 ms² (57%)

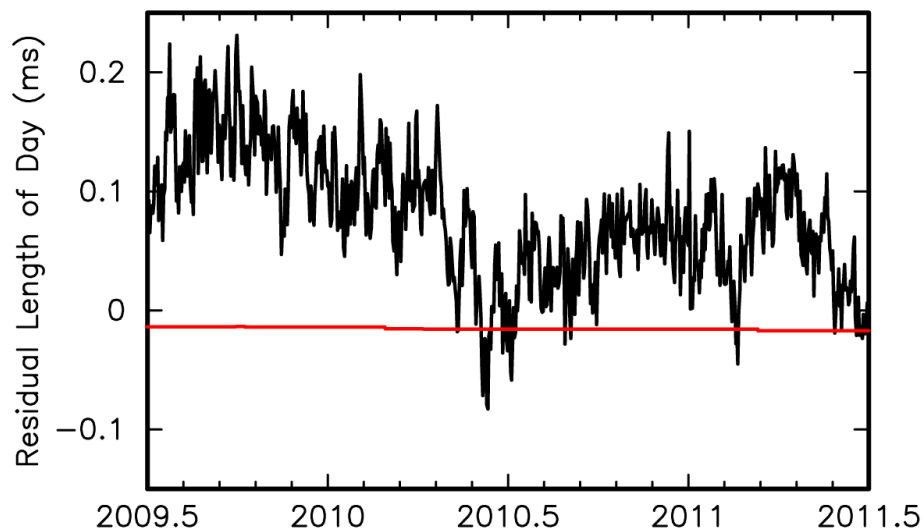
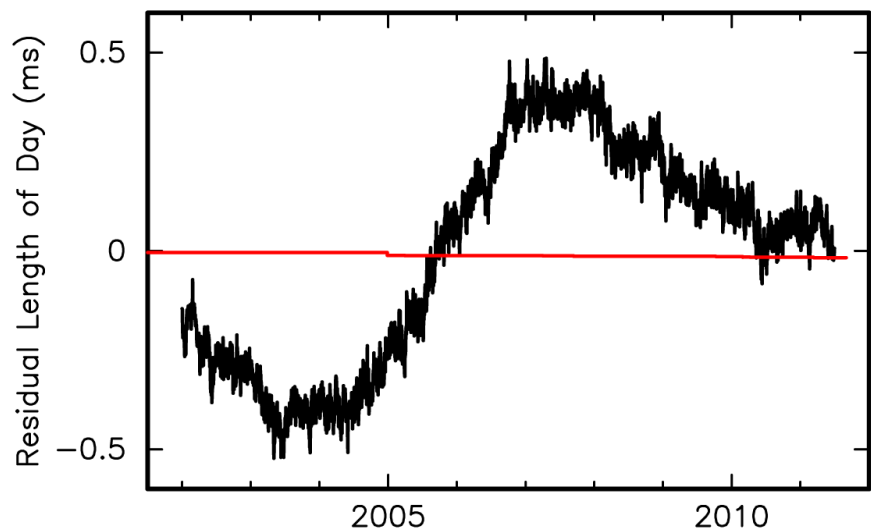
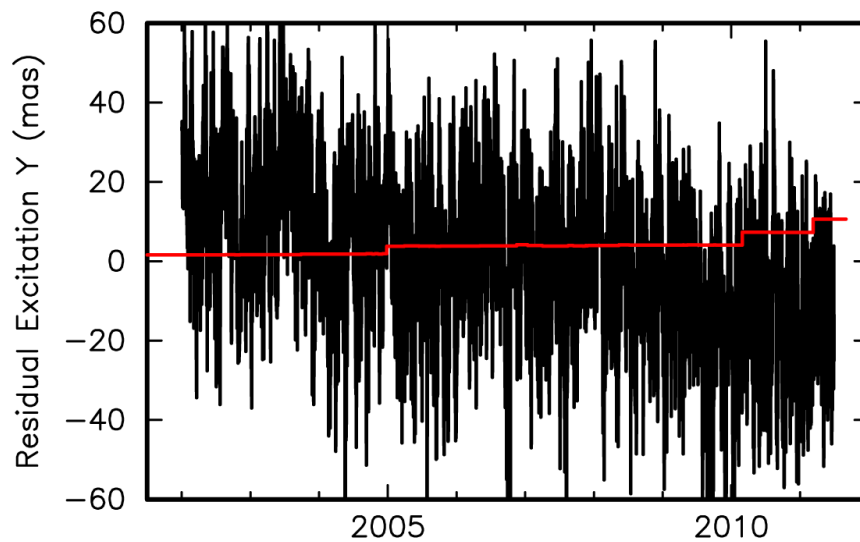
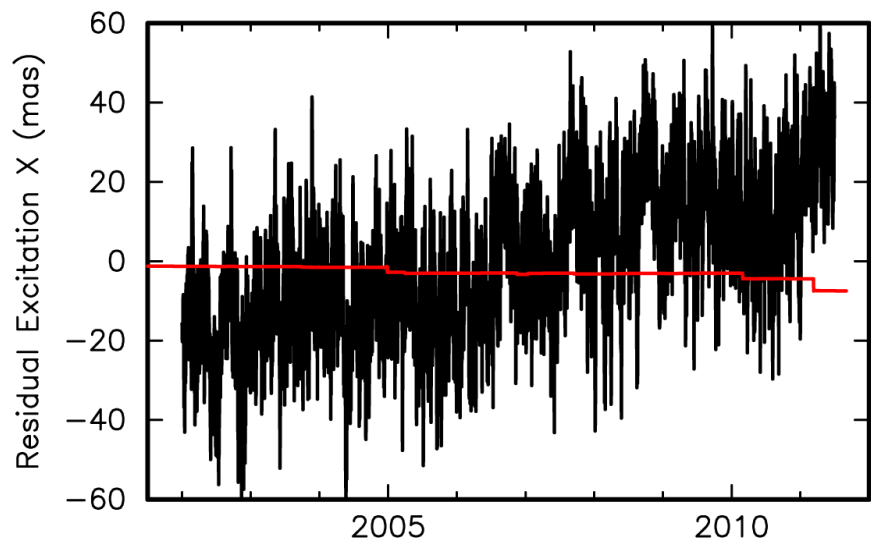
464 mas² (49%)
 532 mas² (73%)
 0.0807 ms² (56%)

394 mas² (57%)
 503 mas² (75%)
 0.0745 ms² (60%)

Modeled Change in Earth Rotation

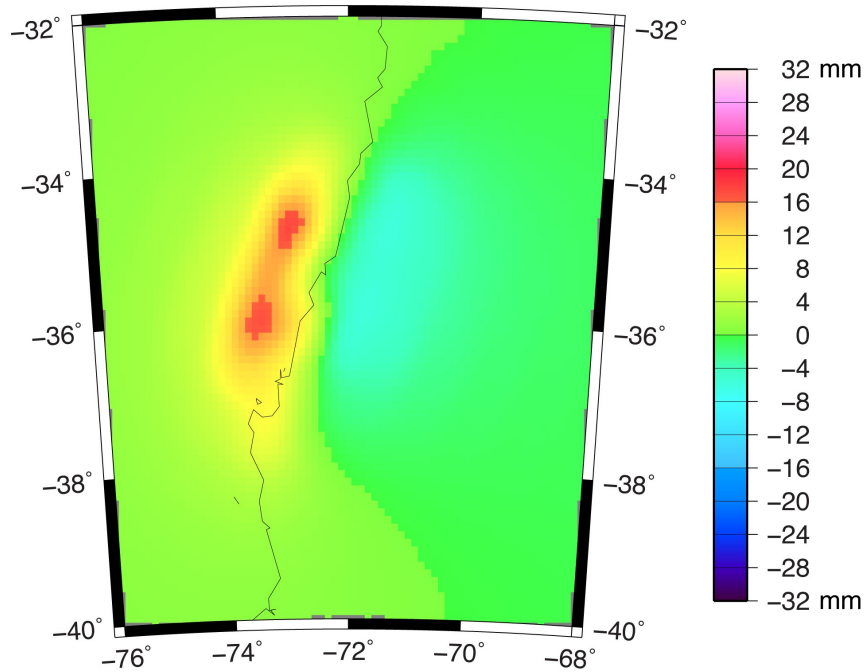


Observed and Modeled Change in Rotation

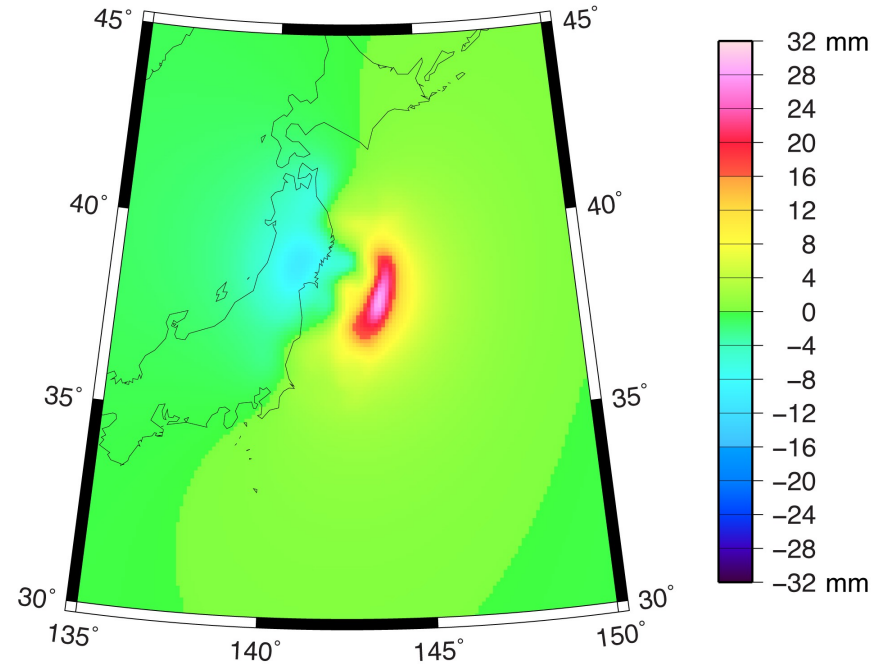


Modeled Change in Geoid

2010 Chile



2011 Japan



Modeled Change in Geopotential

ΔJ_2	ΔJ_3	ΔJ_4	ΔJ_5
(10^{-11})	(10^{-11})	(10^{-11})	(10^{-11})

2004 Sumatran earthquake

2004 Sumatra	$(M_w = 9.3)$	-2.368	-0.621	0.254	0.305
2005 North Sumatra	$(M_w = 8.5)$	-0.283	-0.043	0.034	0.033
2007 South Sumatra	$(M_w = 8.4)$	-0.216	0.000	0.031	0.024
2010 Chile	$(M_w = 8.8)$	-0.302	0.608	-0.263	-0.018
2011 Japan	$(M_w = 9.0)$	0.006	-0.560	-0.343	-0.116

Approximate SLR measurement uncertainty (1σ)

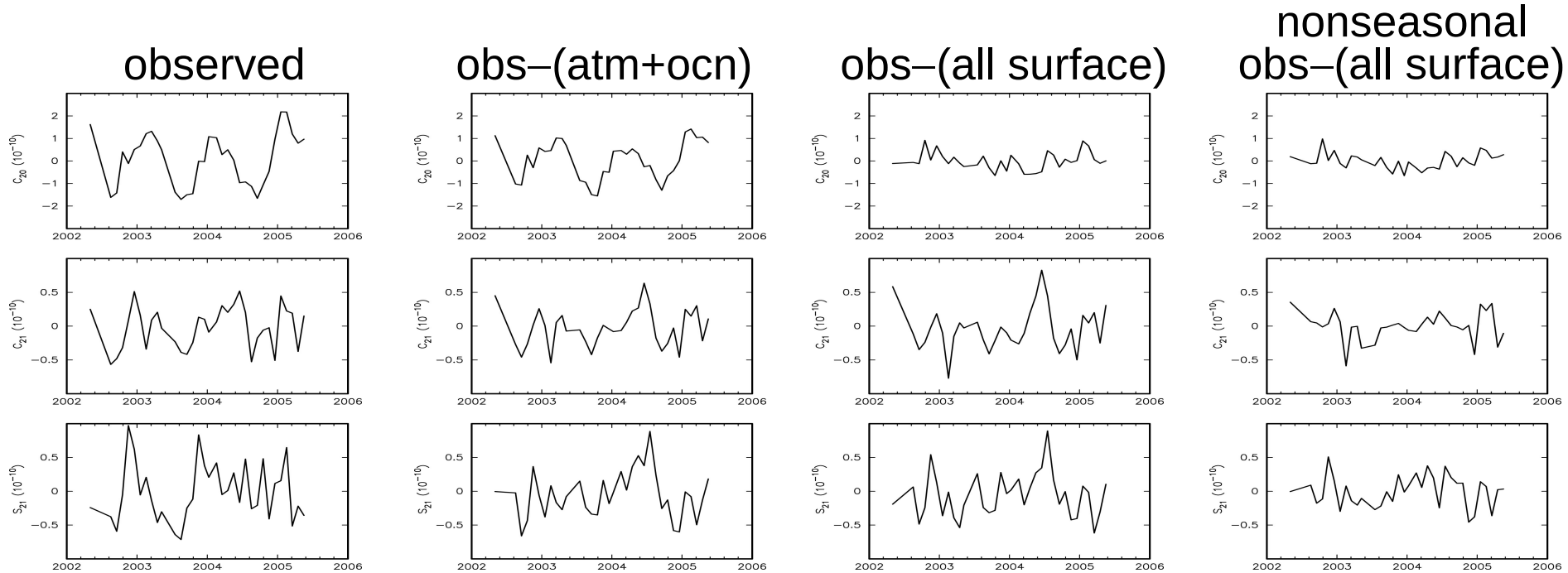
1.3	1.6	4.9
-----	-----	-----

Other great earthquakes

1960 Chilean	$(M_w = 9.5; \text{Chao \& Gross, 1987})$	-0.83	3.29	-1.89	3.64
1964 Alaskan	$(M_w = 9.2; \text{Chao \& Gross, 1987})$	5.25	2.35	1.40	1.62

$$\Delta J_l = -\sqrt{2l+1} \Delta C_{l0}$$

Observed Residual Potential Coefficients from Satellite Laser Ranging (2002.3 – 2005.4)

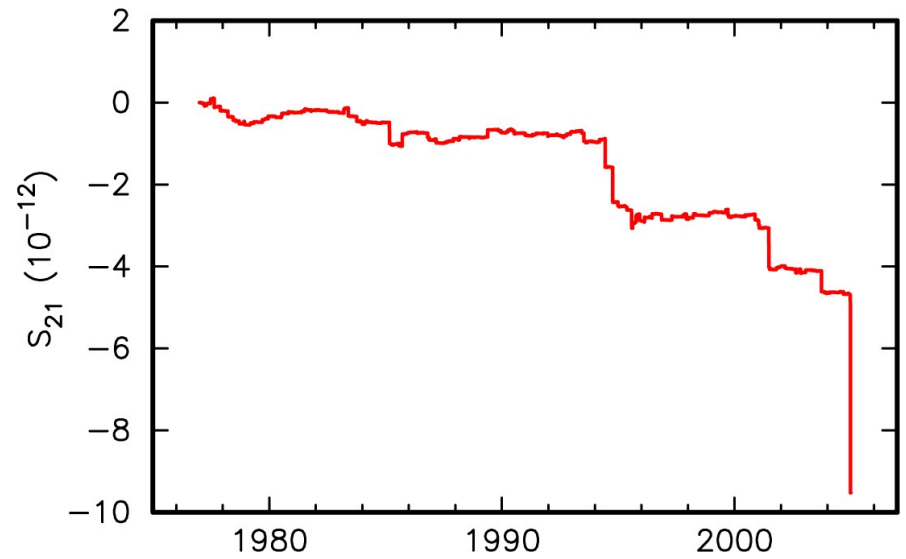
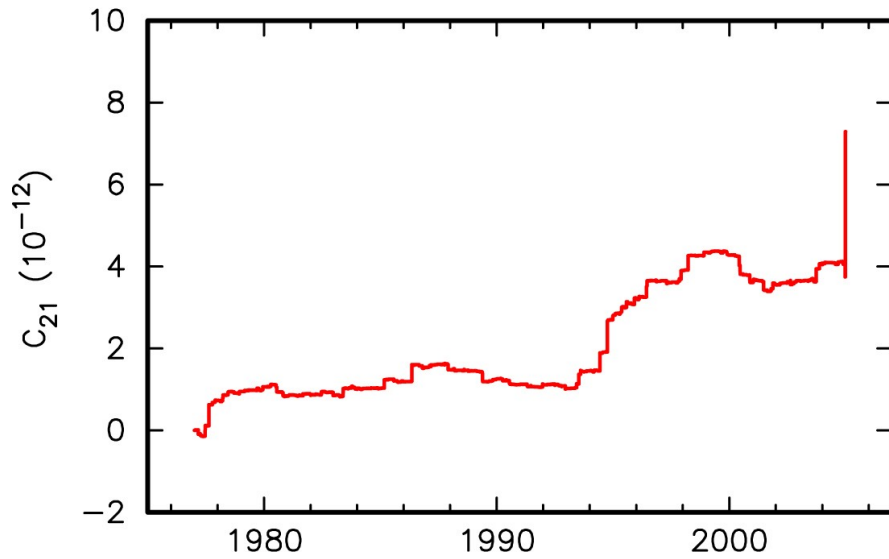
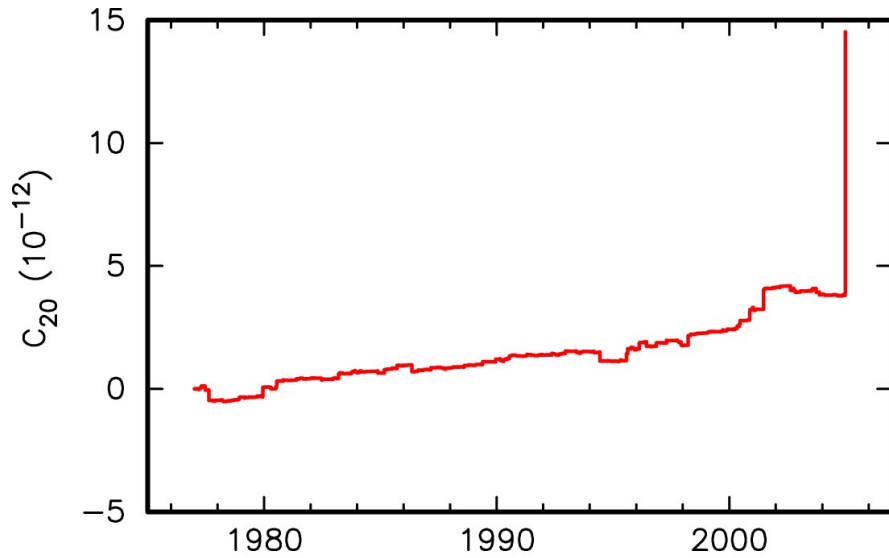


Variance (percent reduction)

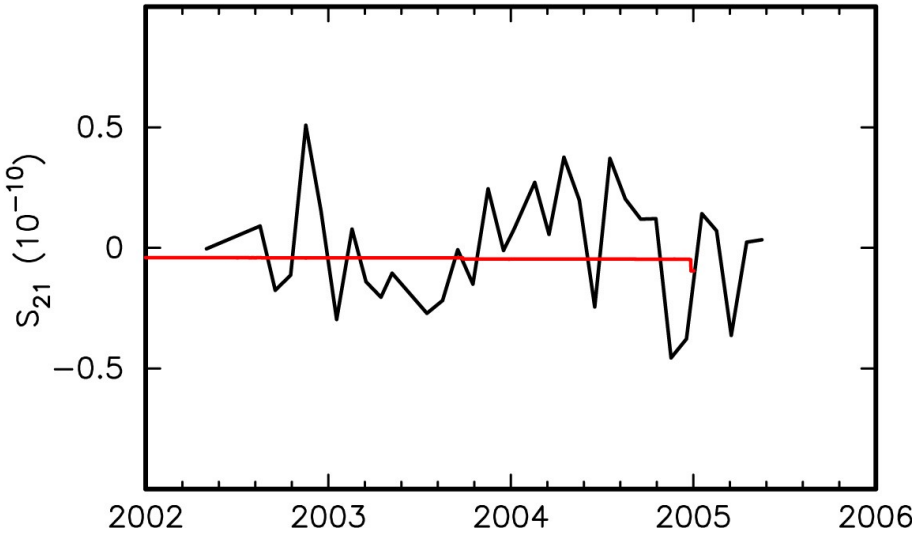
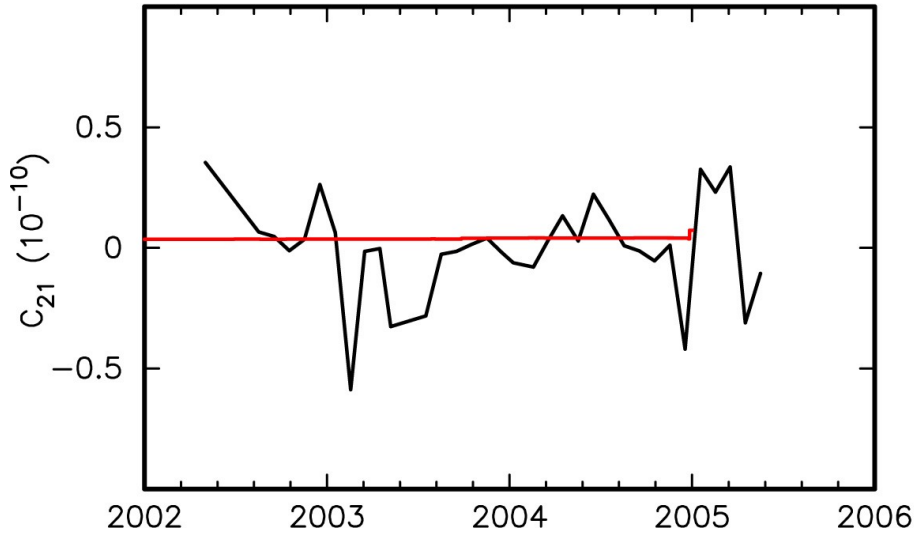
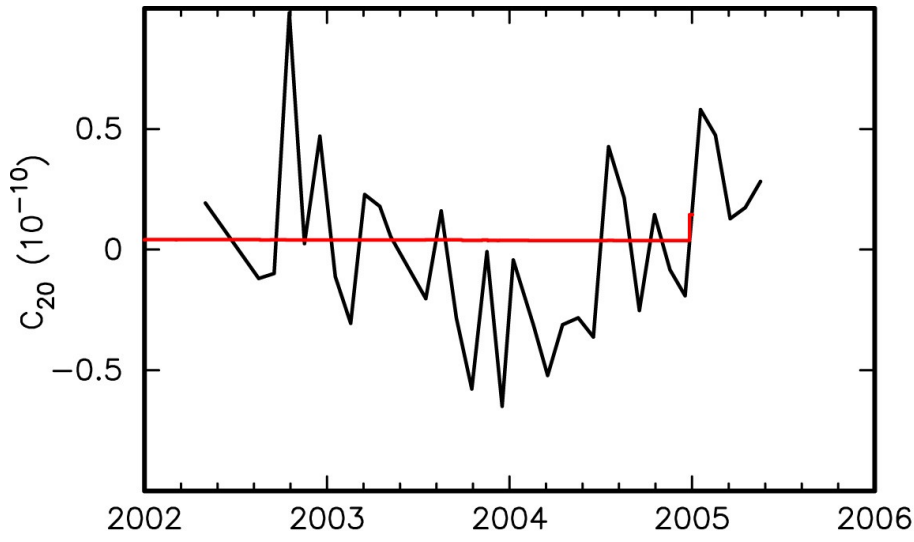
C_{20} :	134.55	72.94 (46%)	15.74 (88%)	12.32 (91%)
C_{21} :	9.73	7.64 (21%)	10.30 (-6%)	4.22 (57%)
S_{21} :	18.30	11.70 (36%)	10.55 (42%)	5.28 (71%)

units of variance: 10^{-22}

Modeled Change in Geopotential



Observed and Modeled Change in Potential



Summary

- Changes in Earth's shape, rotation, and gravity
 - Are measured by the same observing system
 - SLR, GPS, DORIS, VLBI (shape and rotation)
 - Often have a common cause
 - Atmosphere, oceans, hydrology, earthquakes, global isostatic adjustment
 - But are sometimes modeled separately
 - Flat Earth models for earthquake displacements, spherical for rotation
- Unified model
 - Allows common shape, rotation, and gravity observations to be used to determine model parameters
 - Allows consistent geodetic modeling of
 - Surface change
 - Mass transport and exchange
 - Angular momentum exchange

Summary, cont.

- Earthquakes redistribute the Earth's mass on a global scale
 - Change the Earth's rotation and gravitational field
- Greatest earthquakes have greatest effect
 - 1960 Chile
 - 23 mas change in polar motion excitation
 - 8 μ s change in length of day
- Current observing systems are accurate enough to detect changes caused by next great earthquake
 - Polar motion excitation accuracy about 5 mas
 - LOD accuracy about 10 μ s